Canadian Mineralogist
Vol. 28, pp. 321-328 (1990)

DISTRIBUTION OF CATIONS AMONG THE OCTAHEDRA OF PHYLLOSILICATES: INSIGHT FROM EXAFS

ALAIN MANCEAU

Laboratoire de Minéralogie-Cristallographie, Universités Paris 6 et 7, CNRS UA09,
Tour 16, 2ème Étage, 4, place Jussieu, 75252 Paris Cedex 05, France

ABSTRACT

Several recent spectroscopic studies have shown that cations are not always ordered or randomly distributed at the scale of crystallographic sites within the octahedral sheet of phyllosilicates. This paper explains how such a quantitative analysis of the local distribution of cations in phyllosilicates can be realized by EXAFS (Extended X-ray Absorption Fine Structure) spectroscopy. EXAFS evidence of a departure from a random distribution of 3*d* cations is then given for trioctahedral Fe–Mg and Ni–Mg series. In the latter system, the size of Ni clusters (mean size > 20–30 Å) and their widespread presence in natural minerals necessitate a revision of the well-established concept of the Ni–Mg solid solution.

Keywords: EXAFS, phyllosilicates, mica, phlogopite, biotite, "kerolite", site occupancy, Ni–Mg clusters, Fe–Mg distribution.

SOMMAIRE

Plusieurs études spectroscopiques récentes ont montré que les cations ne sont pas toujours ordonnés ou distribués de façon aléatoire à l'échelle de la dizaine d'ångströms dans la couche octaédrique des phyllosilicates. Cet article explique comment une analyse quantitative de la distribution des cations dans les phyllosilicates peut être réalisée par spectroscopie EXAFS (Extended X-Ray Absorption Fine Structure). Deux exemples d'écarts à la distribution aléatoire des cations octaédriques dans les séries trioctaédriques Fe–Mg et Ni–Mg sont ensuite donnés. Dans ce dernier système, la taille des groupements de Ni (taille moyenne > 20-30 Å) et leur généralité dans les minéraux naturels nécessitent une révision du concept de solution solide Ni–Mg.

Mots-clés: EXAFS, phyllosilicates, mica, phlogopite, biotite, "kérolite", occupation de site, domaines Ni–Mg, distribution Fe–Mg.

INTRODUCTION

For several years, there has been a growing awareness that solid solutions, which were considered to be random, have in fact a heterogeneous structure on a very fine scale. These discoveries are mainly due to the emergence of spectroscopic methods, which provide chemical and, in some instances, structural information on the solid solution in the vicinity of the probed element, in contrast to diffraction methods, which are sensitive to the average structure of minerals.

Departure from the random distribution of cations in the octahedral sheet of phyllosilicates has been recognized in dioctahedral micas by nuclear magnetic resonance (NMR) and infrared absorption spectroscopy (IR) (Kalinichenko *et al.* 1975, Sanz & Stone 1979, 1983a,b), in dioctahedral micas by IR (Slonimiskaya *et al.* 1986), and in Ni–Mg "kerolite" (a term not yet formally sanctioned by the IMA and used to describe a phase intermediate between stevensite and talc; *cf.* Brindley *et al.* 1977), also by IR (Gérard & Herbillon 1983). Recently, Manceau and coworkers (Manceau & Calas 1983, 1985, 1986, Decarreau *et al.* 1987, Manceau *et al.* 1988) have applied EXAFS (Extended X-ray Absorption Fine Structure) spectroscopy to the study of the intracrystalline distribution of cations in clay minerals; several new clusterings have been demonstrated in clay minerals containing Ni–Mg and Ni–Fe–Mg.

Applications of EXAFS spectroscopy to solid-state physics and chemistry are relatively new; as a structural tool, it has been in use only for the past 10 years, owing to the availability of synchrotron radiation sources. The EXAFS technique examines the variation of the absorption of X rays with wavelength, extending out from the absorption edge (*K, L* edges) to higher energies by up to ~ 1 keV. The absorption coefficient usually shows a ripple, from which, with suitable processing of the data, information on local structure (*e.g.*, bond distances, number and type of near neighbors) may be obtained. Explanations of the origin of the ripple will not be attempted here; readers in search of theoretical details are referred to recent books or general reviews on this subject (Lee *et al.* 1981, Hayes & Boyce 1982, Stern & Heald 1983, Teo 1986). Suffice it to say here that the EXAFS phenomenon is related to the wave properties of the electron. The ionized photoelectrons interact with neighboring atoms in the solid, which then act as secondary sources of scattering for the photoelectrons. Interference between adjacent scattered waves may occur; this interference influences the probability of absorption of an incident X-ray photon. EXAFS can, therefore, be considered a type of *in situ* electron diffraction in which the source of the electron is the actual atom, which participates in the X-ray absorption event. Using Fourier transform techniques, it is possible to analyze the ripple pattern in order to obtain a radial distribution function (RDF). Unlike diffraction techniques, which give only a single averaged RDF for all the elements present, the RDF obtained from an EXAFS analysis is centered on the X-ray absorber; by tuning to the absorption edge of each element present in the material, a partial RDF for that element may be constructed. The main advantages of EXAFS spectroscopy are its chemical selectivity (all elements are spectroscopically active), and its sensitivity to the local structure (2-5 Å) around the X-ray absorber. These properties make EXAFS particularly well suited for poorly crystalline and non-crystalline materials, and its mineralogical applications encompass Fe and Mn oxides, silicates and glasses. Several recent reviews have been dedicated to the many mineralogical applications of X-ray absorption spectroscopy, and include exhaustive references (Calas *et al.* 1986, 1987, Brown *et al.* 1988, Calas *et al.* 1988, Manceau & Calas 1989, Manceau 1989). In contrast to many other techniques, the structural information extends beyond the immediate coordination shell of the X-ray absorber. Structural information provided by shells of nearest cations make studies of the intracrystalline distribution of elements possible.

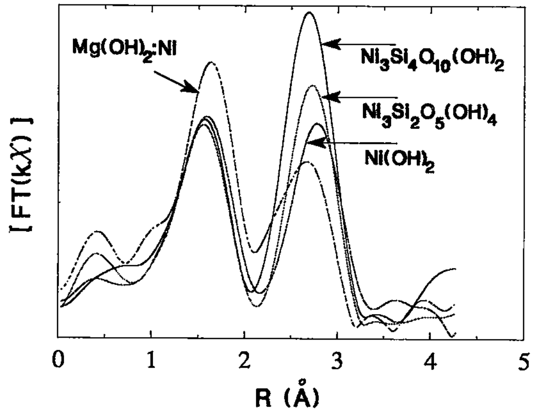

FIG. 1. Radial distribution functions (RDF) at the Ni *K*-edge of $Ni(OH)_2$, $Mg(OH)_2$:Ni, $Ni_3Si_4O_{10}(OH)_2$ and $Ni_3Si_2O_5(OH)_4$.

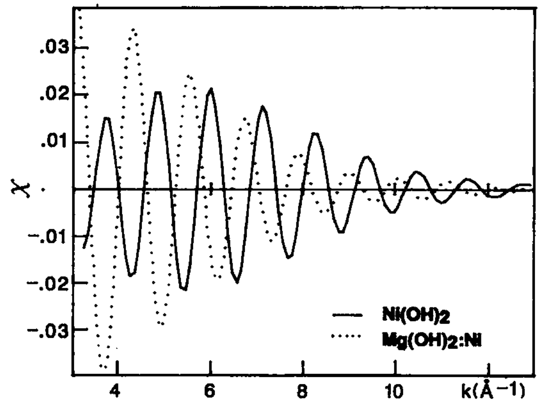

FIG. 2. Fourier-filtered contribution to EXAFS of the nearest shell of cations in $Ni(OH)_2$ and $Mg(OH)_2$:Ni.

This paper shows how a quantitative analysis of the cationic environment around a probed octahedrally coordinated atom can be carried out in phyllosilicates by EXAFS. More generally, the aim of this paper is to make the reader more aware of some real strengths, but also some specific limitations, of this technique as a practical complement to other spectroscopic methods and X-ray crystallography in the study of the real nature of solid solutions in phyllosilicates.

PRESENCE OF A UNIQUE SHELL OF NEAREST CATIONS

Sinusoidal EXAFS oscillations are caused by the interference term $\sin[2kr_j + \phi(k)]$. Here, k is the photoelectron wave vector, r_j, the distance of the atomic shell j, and $\phi(k)$, the total phase-shift associated to the absorber – back-scatterer pair. Determination of the nature of the cations that are the nearest neighbors surrounding the X-ray absorber, and hence of the distribution of cations, takes advantage of the fact that the scattering phase-shifts of 3*d* [$\phi_{3d}(k)$] elements and of Mg, Al and Si [$\phi_{Mg,Al,Si}(k)$] are known to differ by about π (Teo & Lee 1979). A destructive interference occurs between waves back-scattered by "heavy" and "light" elements, provided the atomic shells are equidistant (*i.e.*, $r_{3d} \approx r_{Mg,Al,Si}$). This condition is most often fulfilled in minerals in the case of atomic substitution, which renders EXAFS particularly sensitive to the chemical composition of the nearest shell of cations.

A favorable example is provided by the Mg-Ni solid solution since, owing to the similarity in ionic radius of Mg^{2+} and Ni^{2+}, there is no significant structural distortion along the series. Ni *K*-RDF of $Ni(OH)_2$ and $Mg(OH)_2$ doped with Ni [$Mg(OH)_2$:Ni] are displayed in Figure 1. Both functions present two intense peaks associated with the first anion and cation atomic shells. Because of the presence of the phase-shift function $\phi(k)$ within the interference term, each peak is shifted from the true distance r_j by an amount that depends on the atomic pair under consideration. At this stage of the analysis, a Fourier transform of a selected peak yields the contribution of this isolated atomic shell to the EXAFS. The result of this operation, performed for the cationic contribution to EXAFS of $Ni(OH)_2$ and $Mg(OH)_2$:Ni (second RDF peaks), is reported in Figure 2. Both curves are almost exactly out of phase by 180° over most of their energy span. This result stems from the fact that Ni is surrounded by 6Ni in $Ni(OH)_2$ and 6Mg in $Mg(OH)_2$:Ni at a similar distance (3.09–3.13 Å; this work and Brindley & Kao 1984) The simultaneous presence of Ni and Mg, and more generally of "light" and "heavy" atoms, in the second coordination shell of a mineral will result in a destructive interference. A complete cancellation of waves would be observed with a nearest cation shell filled by 4Mg + 2Ni. These curves also differ in their magnitude in the whole k range. For light elements, the scattering amplitude function decreases monotonically with k, whereas for $3d$ elements, a peak progressively appears from the low-k region as Z increases (Teo & Lee 1979).

INTERFERENCE BETWEEN NEAREST AND NEXT-NEAREST CATION SHELLS

Evidence for such an interference in sheet silicates

The second RDF peaks of the nickeliferous talc [$Ni_3Si_4O_{10}(OH)_2$] and the nickeliferous serpentine [$Ni_3Si_2O_5(OH)_4$] are enhanced compared to that of $Ni(OH)_2$, even though in these three structures Ni atoms are surrounded by 6Ni at about the same distance (Fig. 1). Ni-cation contributions to EXAFS obtained by the Fourier transformation also differ by their amplitude envelope (Fig. 3). The difference between the amplitude of these sinusoids decreases monotonically with k; this result lends credence to the additional contribution of a low-Z element in the EXAFS spectra of phyllosilicates. A good spectral fit can only be obtained by adding the contribution of the nearest Si atoms, located at 3.21 Å, just beyond the first Ni shell (3.00 Å; Fig. 4). In that mineral, the difference in distance (ΔR = 0.2 Å) cancels out the difference in phase shift between Si and Ni over most of the k span ($2k\Delta R = \phi_{Ni} - \phi_{Si} \approx \pi$), and thereby enhances the resultant wave, and hence, the second RDF peak. The difference in magnitude of this second RDF peak in the nickeliferous talc and serpentine arises from the fact that in the *TOT* and *TO* structures, the number of nearest Si is equal to 4 and 2, respectively. It turns out that in phyllosilicates, the nearest EXAFS contribution of the sheet(s) of tetrahedra is mostly hidden by that of the sheet of octahedra; omission of the cation–(Si,Al) atomic pair (Fukushima & Okamoto 1987, Güttler *et al.* 1989) would result in an overestimation of the number of "heavy" elements.

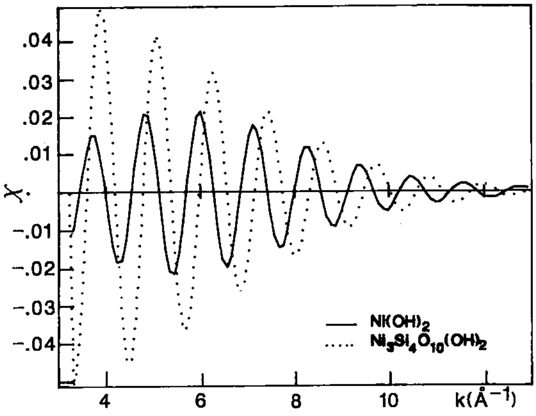

FIG. 3. Fourier-filtered contribution to EXAFS of nearest shell of cations in $Ni(OH)_2$ and $Ni_3Si_4O_{10}(OH)_2$. For clarity, the Ni-cation contribution of $Ni_3Si_2O_5(OH)_4$ has not been plotted. It ranges between those of $Ni_3Si_4O_{10}(OH)_2$ and $Ni(OH)_2$.

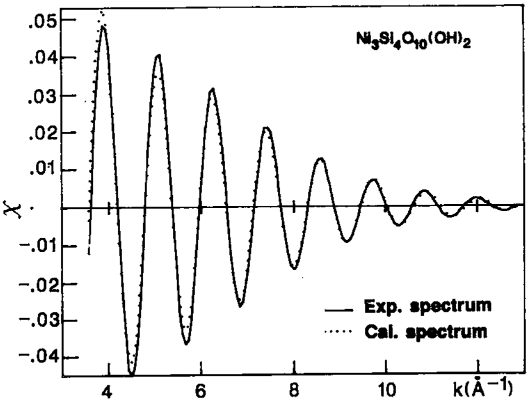

FIG. 4. Spectral fitting of contributions by the nearest and next-nearest cations to EXAFS in $Ni_3Si_4O_{10}(OH)_2$. The calculated curve corresponds to 6Ni neighbors at 3.00 Å (σ = 0.09 Å, γ = 1.00 $Å^{-2}$) and 4Si neighbors at 3.21 Å (σ = 0.08 Å, γ = 1.05 $Å^{-2}$).

The fact that the sheet of octahedra in phyllosilicates can simultaneously be filled by transition element, Mg and Al atoms complicates the interpretation of spectra, leading to a multiplicity of mathematical solutions during the fitting procedure (Manceau & Decarreau 1988). For a given structure, one may reasonably postulate that the contribution of tetrahedra to EXAFS is independent of the chemical composition of the sheet of octahedra. If one were able to filter it, it would be possible to subtract this contribution from the EXAFS spectrum of a wide range of structurally related phyllosilicates. Such an operation should permit, in turn, a more accurate analysis of the true structure of solid solu-

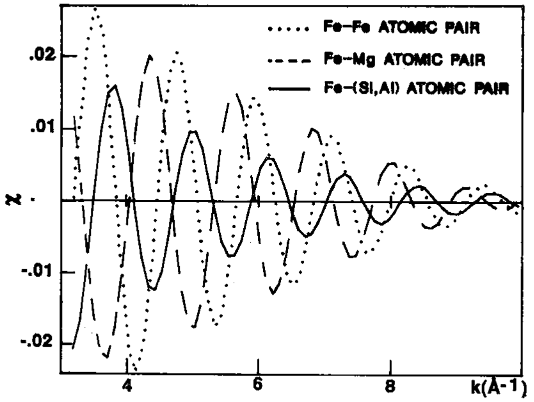

FIG. 5. Elementary cation–cation contributions in phyllosilicates. Solid line: Fe–(Si,Al); dashed line: Fe–Mg; dotted line: Fe–Fe. Contributions reported herein are those of a powder spectrum.

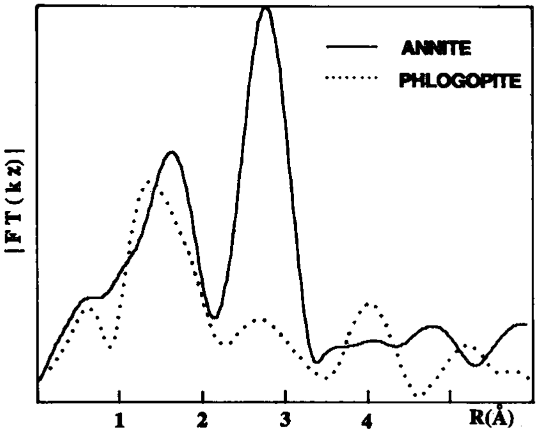

FIG. 6. Radial distribution functions (RDF) of annite and phlogopite given for powder EXAFS spectra.

tions. Such a selectivity among pairs of atoms can be achieved, in favorable cases, by using the plane-polarization nature of the synchrotron beam (Manceau *et al.* 1988).

Filtering cation–cation contributions

The angular dependence of EXAFS is given by:

$$\chi(k,\theta) = \sum_j 3 < \cos^2\theta_j > \chi_j(k)$$

where j is the number of the neighboring atomic shell, $\chi_j(k)$ is the isotropic contribution of the j^{th} shell, and θ_j is the angle between the electric field vector and the absorber–scatterer vector. When the electric field vector is out of the plane of the layers in a single crystal, the contribution of the octahedral sheet is zero, and the Fe–(Si,Al) pair is selected. Going further in the spectral analysis, by knowing the tetrahedral contribution in the out-of-plane position, it is possible to calculate its contribution to the in-plane position of a single crystal ($\theta = 57°$) or in a powder spectrum, and hence, to subtract it to obtain the contribution of octahedra. In order to decipher how elementary waves interfere in trioctahedral micas, this operation has been carried out first on a phlogopite single crystal [Fe/(Fe + Mg) = 0.07], which yields the Fe–(Si,Al) and the Fe–Mg contributions to EXAFS. The Fe–Fe contribution was then isolated from the annite spectrum after subtraction of the (Si,Al) contribution.

Results are shown in Figure 5. Here the difference in distance between Mg and (Si,Al) shells in phlogopite shifts the photoelectron waves by $\pi(\phi_{Mg} \approx \phi_{Al,Si}$, and $\Delta R \approx 0.23$ Å). Owing to this phase cancellation, the second RDF peak of the phlogopite powder EXAFS spectrum decreases in amplitude but does not vanish, because the number of Mg and (Si,Al) neighbors is not equal (6 *versus* 4, Fig. 6). Fe–Fe and Fe–(Si,Al) contributions are shifted by $\approx \pi/2$. This effect stems from a combined effect of phase-shift difference (ϕ_{Fe}–$\phi_{Si,Al} \approx \pi$; after Teo & Lee 1979) and incoherence of Fe–Fe and Fe–(Si,Al) distances (d[Fe–Fe] = 3.10–3.12 Å, d[Fe–Si,Al] = 3.28 Å): $2k\Delta R + \Delta\phi \approx \pi/2$.

The amplitude envelope of the Fe–Fe contribution monotonically decreases, and hence, is different from that expected for a single 3d atomic shell. The same explanation used before for the nickeliferous talc, *i.e.*, additional contribution of a low-Z element, also is applied here. The responsible atomic pair is probably ^{IV}Fe–^{IV}Si, as a Mössbauer study of this sample of annite revealed that 9.1 at.% of Fe atoms are tetrahedrally coordinated.

APPLICATION: DISTRIBUTION OF CATIONS WITHIN THE SHEET OF OCTAHEDRA IN PHYLLOSILICATES

Ni–Mg-bearing phyllosilicates

Figure 7a shows the Fourier-filtered Ni–(Ni,Mg,Si) contributions of two samples of Ni-containing "kerolite" from Yugoslavia (Maksimovic 1966). The amplitudes of these two contributions are roughly similar, even though one sample is ten times less rich in nickel than the other. This result indicates that the chemical composition of the nearest octahedral shell is quite independent of the Ni-content of "kerolite", as the presence of Mg neighbors would have lessened the wave amplitude (waves back-scattered by Mg and Ni are out of phase). To date, Ni clusterings have been identified in all natural Ni-containing phyllosilicates studied, whatever their nature ("kerolite", lizardite, sepiolite, smectite and chlorite) and origin (New Caledonia: Manceau & Calas 1983, 1985, 1986; Brazil: Decarreau *et al.* 1987; Yugoslavia: Manceau 1989). A quantitative analysis has shown that the deviation from the statistical distribution of Ni and Mg atoms is important (Fig. 8), and that the average size of $Ni(O,OH)_6$ clusters is always greater than 20–30 Å. Their upper limit is not yet known. Are Ni segregations embedded in Ni–Mg layers, or do they build pure Ni layers intimately mixed with Mg layers? Infrared spectroscopic studies (Gérard & Herbillon 1983, Brindley *et al.* 1979) have demonstrated the existence of large amounts of NiNiMg associations, whereas NiMgMg ones are always few. These results indicate that all the Ni-rich clusters, or at least the majority of them, are embedded within Ni–Mg sheets. Given the generality and size of Ni segregations in natural clays, an interesting second question then arises as to whether or not Ni–Mg phyllosilicates can always be regarded as members of a solid solution extending from Mg and Ni end-members. Should Ni–Mg-bearing clay minerals not be regarded as a two-phase mixture of the end members? In other words, what is the minimum size of Ni domains that is required in order to consider them as inclusions of the pure Ni phase within the Mg layer instead of a perturbation of the ideal solid-solution? Until now, all attempts to accurately determine the actual structure of Ni–Mg-bearing clays by HRTEM and STEM have failed owing to technical difficulties.

Fe–Mg micas

Sanz & Stone (1979, 1983a,b) have shown by NMR and IR that the distribution of Fe and Mg in the phlogopite–annite series is not random. Figure 7b compares the contribution of the Fe–cation pairs of three micas [samples B1, B8 and NB in Sanz & Stone (1978, 1983a,b)]. The wave amplitude of sample NB is lower than that of B1 because of the presence of a greater amount of Mg instead of Fe as nearest neighbor. This result is in agreement with the results of a chemical analysis, since NB is depleted in Fe. Of significance is the closeness of B1 and B8 spectra, which indicates a similar chemical environment around Fe atoms in spite of the fact that B1 is roughly twice as rich in Fe as is B8. This result clearly points to the fact that the distribution of Fe and Mg in the sample B8 is not random, and agrees with NMR results. This preliminary study of the phlogopite–annite series is ongoing, with the aim of comparing the efficiency of both NMR and EXAFS spectroscopies in probing into the real structure of phyllosilicates.

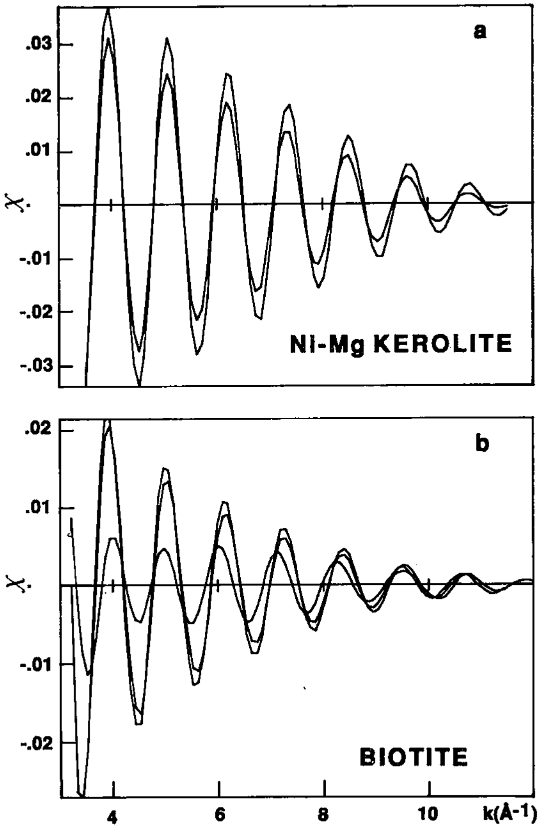

FIG. 7. Evidence of a nonrandom distribution of Ni and Fe atoms within the octahedra of phyllosilicates. a) Fourier-filtered Ni–(Ni,Mg,Si) contributions in Ni-containing "kerolite" from Yugoslavia (Maksimovic 1966). In decreasing wave amplitude, Ni/(Ni + Mg) = 0.41 and Ni/(Ni + Mg) = 0.04. b) Fourier-filtered Fe–(Fe,Mg,Si,Al) contributions. In decreasing wave amplitude, samples B8, B1 and NB with a ratio (ΣHeavy cations/ΣOctahedral cations) equal to 0.54, 0.33 and 0.13, respectively.

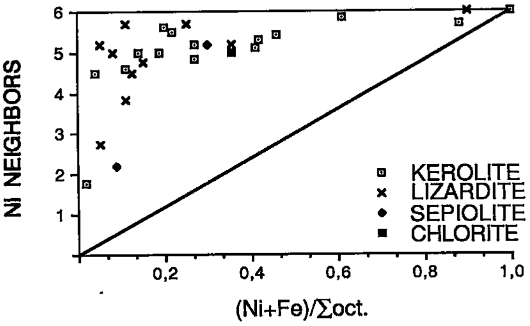

FIG. 8. Deviation from the statistical distribution of Ni atoms in phyllosilicates. The intensity of this deviation is independent of the mineral species and occurrence. Points reported herein have been collected from Manceau & Calas (1986) and Manceau (1989).

DISCUSSION: LIMITATIONS OF EXAFS SPECTROSCOPY FOR THE SPECIFIC STUDY OF PHYLLOSILICATES

Even though this paper demonstrates the usefulness of EXAFS for probing the detailed structure of clay minerals, difficulties encountered in the quantitative interpretation of the information provided by nearest cationic shells in such multielement materials must not be underestimated. Among the major limitations inherent to this technique in regard to the study of phyllosilicates are: (i) the difficulty in discriminating elements with similar atomic numbers; (ii) the existence of site multiplicity of the X-ray absorber; (iii) the presence of octahedral vacancies in dioctahedral structures; (iv) the necessity of having well-known samples from which phase shifts and amplitude functions will be extracted; (v) the existence of a preferential orientation of layer particles (texture effect), and (vi) the overlap between the contributions to EXAFS of the sheets of octahedra and tetrahedra.

The first limitation precludes discrimination between Mg and Al, on one hand, and Ti, Fe and Ni, on the other, among second neighbors. It is a severe drawback because most of the poorly crystallized clays are multielement materials. In the case where the probed element would occupy several crystallographic sites, EXAFS will provide its averaged short-range order. This requirement of a unique site-occupancy also reduces the number of minerals that can be studied by this technique, because several cations generally fill simultaneously 4-fold- and 6-fold-coordinated sites (*e.g.*, Al and Fe^{3+} in many dioctahedral clays). The presence of octahedral vacancies is also a severe handicap because the total number of nearest cations is then not known. For instance, since Fe atoms are roughly twice as heavy as (Mg,Al) and waves back-scattered by each of them are out of phase, the contributions to EXAFS of atomic shells filled with $4Fe^{2+} + 2(Mg,Al)$ or $3Fe^{3+}$ are virtually identical (Fig. 9). These two atomic arrangements being indistinguishable by EXAFS, complementary spectroscopic and diffraction studies are required. This remark points to the impossibility for EXAFS spectroscopy to be able to study accurately the local order of clay particles suspected to be structurally intermediate between trioctahedral and dioctahedral series. The fourth limitation may be easily overcome owing to the availability of well-known reference materials over a large range in composition. Owing to the plane-polarized nature of the synchrotron beam, texture effects may strongly affect the amplitude of the signal, and prevent any reliable quantification of the degree of order or disorder of cations (Manceau *et al.* 1988). These effects can be always circumvented by rotating the imperfectly disoriented powder by 35° about an axis perpendicular to both the electric field vector *E* and the beam direction (Manceau *et al.* 1990). The sixth limitation extends to close-packed structures in which first- and second-nearest cations are located at about the same distance from the central atom, as their contributions could not be filtered by the Fourier transform. This difficulty may be surmounted, once again, taking advantage of the plane polarization of the synchrotron beam as, in addition to the chemical selectivity of EXAFS, the specific contribution

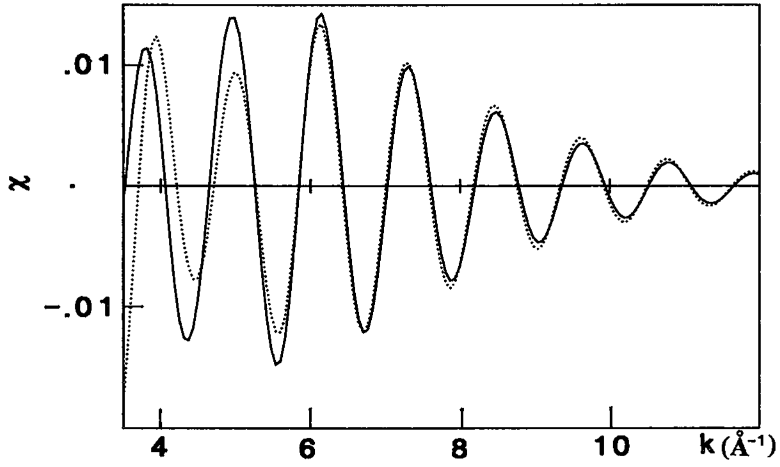

FIG. 9. Simulations of the contributions to EXAFS of two different shells of cations. Full line: 3Fe at 3.05 Å; dotted line: 4Fe + 2Mg at 3.05 Å. For both simulations: $\sigma = 0.08$ Å, $\gamma = 1.00$ Å^{-2}. These $\chi(k)$ functions have been calculated using amplitude and phase-shift values tabulated by Teo & Lee (1979).

of a given atomic pair can be selected by orienting a single crystal in the X-ray beam. For these reasons, powder EXAFS spectra of silicates are extremely difficult to interpret beyond the first coordination sphere, inasmuch as the mathematical solution never is unique (Manceau & Decarreau 1988). In view of these complex structural problems, studies of the intracrystalline distribution of major elements and impurities by EXAFS are, still today, restricted to trioctahedral phyllosilicates because all their octahedra are filled, and their low symmetry makes angular analysis feasible.

If one is aware of these limitations, EXAFS spectroscopy can be used as a powerful tool for the analysis of the intracrystalline distribution of elements in minerals. Several studies have already put forward the mosaic structure of clay minerals down to the layer scale. Reasons for such segregations of cations are considered to lie mainly in nonequilibrium processes that prevail during crystal growth at low temperature.

ACKNOWLEDGEMENTS

A. Decarreau, M. Volfinger, J. Sanz and W.E. Stone are kindly thanked for providing the phyllosilicates samples. The help of R.F. Martin in polishing the English is acknowledged.

REFERENCES

BRINDLEY, G.W. & KAO, C.C. (1984): Structural and IR relations among brucite-like divalent metal hydroxides. *Phys. Chem. Miner.* **10**, 187-191.

______, BISH, D.L. & WAN, H.M. (1977): The nature of kerolite, its relation to talc and stevensite. *Mineral. Mag.* **41**, 443-452.

______, ______ & ______ (1979): Compositions, structures and properties of nickel-containing minerals in the kerolite–pimelite series. *Am. Mineral.* **64**, 615-625.

BROWN, G.E., JR., CALAS, G., WAYCHUNAS, G.A. & PETIAU, J. (1988): X-ray absorption spectroscopy and its applications in mineralogy and geochemistry. *In* Spectroscopic Methods in Mineralogy and Geology (F.C. Hawthorne, ed.). *Rev. Mineral.* **18**, 430-512.

CALAS, G., BROWN, G.E., JR., WAYCHUNAS, G.A. & PETIAU, J. (1987): X-ray absorption spectroscopic studies of silicate glasses and minerals. *Phys. Chem. Miner.* **15**, 19-29.

______, MANCEAU, A. & PETIAU, J. (1988): Crystal chemistry of transition elements in minerals through X-ray absorption spectroscopy. *In* Synchrotron Radiation Applications in Mineralogy and Petrology (S.S. Augustithis, ed.). Theophrastus Publ. S.A., Athens (77-95).

______, PETIAU, J. & MANCEAU, A. (1986): X-ray absorption spectroscopy of geological materials. *J. Physique* **C8**, 813-818.

DECARREAU, A., COLIN, F., HERBILLON, A., MANCEAU, A., NAHON, D., PAQUET, H., TRAUTH-BADAUD, D. & TRESCASES, J.J. (1987): Domains segregation in Ni–Fe–Mg-bearing smectites. *Clays Clay Miner.* **35**, 1-10.

FUKUSHIMA, Y. & OKAMOTO, T. (1987): Extended X-ray absorption fine-structure study of cobalt-exchanged sepiolite. *Proc. Int. Clay Conf.* (L.G. Schultz, H. Van Olphen & F.A. Mumpton, eds.). The Clay Minerals Society, Bloomington, Indiana (9-16).

GÉRARD, P. & HERBILLON, A. (1983): Infrared studies of Ni-bearing clay minerals of the kerolite–pimelite series. *Clays Clay Miner.* **31**, 143-151.

GÜTTLER, B., NIEMANN, W. & REDFERN, S.A.T. (1989): EXAFS and XANES spectroscopy study of the oxidation and deprotonation of biotite. *Mineral. Mag.* **53**, 591-602.

HAYES, T.M. & BOYCE, J.B. (1982): Extended X-ray absorption fine structure spectroscopy. *Solid State Phys.* **37**, 173-351.

KALINICHENKO, A.M., MATYASH, L.V., KHOMYAK, T.P. & PAVLISHIN, V.I. (1975): Distribution of octahedral cations in biotites according to the data of proton magnetic resonance. *Geochem. Int.* **12**(1), 18-24.

LEE, P.A., CITRIN, P.H., EISENBERGER, P. & KINCAID, B.M. (1981): Extended X-ray Fine Structure: its strength and limitations as a structural tool. *Rev. Modern Phys.* **53**, 769-806.

MAKSIMOVIC, Z. (1966): βkerolite–pimelite series from Goles Moutain, Yugoslavia. *Proc. Int. Clay Conference (Israel)*, 97-105.

MANCEAU, A. (1989): Étude des argiles par spectroscopie d'absorption X. *In* Les Matériaux Argileux, Structure, Propriétés et Applications (A. Decarreau, ed.). Soc. Fr. Minéral. Cristallogr., Paris (in press).

______, BONNIN, D., KAISER, P. & FRÉTIGNY, C. (1988): Polarized EXAFS of biotite and chlorite. *Phys. Chem. Miner.* **16**, 180-185.

______, ______, STONE, W.E.E. & SANZ, J. (1990): Distribution of Fe in the octahedral sheet of trioctahedral micas by polarized EXAFS. Comparison with NMR results. *Phys. Chem. Miner.* (in press).

______ & CALAS, G. (1983): Short and medium range order in nickeliferous clay minerals by X-ray absorption spectroscopy. *Proc. 5th Meeting European Clay Groups* (J. Konta, ed.). Univerzita Karlova, Praha, Czechoslovakia (547-552).

______ & ______ (1985): Heterogeneous distribution of nickel in hydrous silicates from New Caledonia ore deposits. *Am. Mineral.* **70**, 549-558.

______ & ______ (1986): Ni-bearing clay minerals. 2. X-ray absorption study of Ni-Mg distribution. *Clay Minerals* **21**, 341-360.

______ & ______ (1989): Chemical and structural applications of X-ray absorption spectroscopy in mineralogy. *Nouveau J. Chim. Phys.* **86**, 1533-1546.

______ & DECARREAU, A. (1988): Extended X-ray absorption fine structure study of cobalt-exchanged sepiolite: a comment on the paper by Fukushima and Okamoto. *Clays Clay Miner.* **36**, 382-383.

SANZ, J. & STONE, W.E.E. (1978): The location and content of iron in natural biotites and phlogopites: a comparison of several methods. *Clay Miner.* **13**, 45-52.

______ & ______ (1979): NMR study of micas. II. Distribution of Fe^{2+}, F^-, and OH^- in the octahedral sheet of phlogopites. *Am. Mineral.* **64**, 119-126.

______ & ______ (1983a): NMR study of minerals. III. The distribution of Mg^{2+} and Fe^{2+} around the OH groups in micas. *J. Phys. C: Solid State Phys.* **16**, 1271-1281.

______ & ______ (1983b): NMR applied to minerals. IV. Local order in the octahedral sheet of micas: Fe–F avoidance. *Clay Miner.* **18**, 187-192.

SLONIMISKAYA, M.V., BESSON, G., DAINYAK, L.G., TCHOUBAR, C. & DRITS, V.A. (1986): Interpretation of the IR spectra of celadonites and glauconites in the region of OH-stretching frequencies. *Clay Miner.* **21**, 377-388.

STERN, E.A. & HEALD, S.M. (1983): Basic principles and applications of EXAFS. *In* Handbook on Synchrotron Radiation (E.E. Koch, ed.). North Holland, Amsterdam.

TEO, B.K. (1986): *EXAFS: Basic Principles and Data Analysis.* Inorg. Chem. Concepts Vol. 9, Springer Verlag, New York.

______ & LEE, P.A. (1979): Ab initio calculation of amplitude and phase function for Extended X-ray Absorption Fine Structure (EXAFS) spectroscopy. *J. Am. Chem. Soc.* **101**, 2815-2830.

Received August 28, 1989, revised manuscript accepted February 28, 1990.